

Zilin Chen · Ping Wang · Hsueh-Chia Chang

## An electro-osmotic micro-pump based on monolithic silica for micro-flow analyses and electro-sprays

Received: 30 September 2004 / Revised: 22 January 2005 / Accepted: 25 January 2005 / Published online: 1 April 2005  
© Springer-Verlag 2005

**Abstract** A high-pressure electro-osmotic micro-pump fabricated by a sol-gel process is reported as a fluid-driving unit in a flow-injection analysis (FIA) system. The micro FIA system consists of a monolithic micro-pump on a glass slide (2.5×7.5 cm), a micro-injector, and a micro-sensor (2.5×1.5 cm). The monolithic silica matrix has a continuous skeleton morphology with micrometer-sized through-pores. The micrometer-size pores with a large negative surface charge density build up a large pressure under a DC electric field to drive fluid through the downstream units. A novel Nafion joint for the downstream cathode eliminates flow into the electrode reservoir and further enhances pressure build-up. The measured pump-pressure curve indicated a maximum pressure of 0.4 MPa at flow rate of 0.4  $\mu\text{L min}^{-1}$  at 6 kV. Despite the large voltage, the small current transmission area through the monolith produced a negligible current (less than 100  $\mu\text{A}$ ) that did not generate bubbles or ion contaminants. The flow rate can be precisely controlled in the range 200 nL to 2.5  $\mu\text{L min}^{-1}$  by varying the voltage from 1 to 6 kV. The high pump pressure and the large current-free DC field also enabled the pump to act as an electro-spray interface with a downstream analytical instrument.

**Keywords** Electroosmotic micropump · Monolith · Sol-gel · Bio-sensor · Flow-injection analysis · Electro-spray

### Introduction

Considerable effort in analytical chemistry has been directed toward the miniaturization of total analytical systems (TAS) to enable rapid, portable, and automated analyses of small-volume samples. Ideally, a micro-TAS ( $\mu\text{-TAS}$ ) integrates all function units necessary to analyze a sample on a single micro-fluidic substrate. Because the flow velocity in a micro-channel scales as the channel radius squared, scaling down the system by a factor  $n$  requires an  $n^2$  increase in the driving pressure to maintain the same velocity. As such, a critical component of a  $\mu\text{-TAS}$  is a powerful micro-fluidic pump capable of generating high pressure. Moreover, this pump should ideally be integrated into the entire system on the same substrate. Fluid transfer from an external pump would defeat many of the advantages of  $\mu\text{-TAS}$  and would require tedious tubing connection for each run. Constant high-pressure but low flow rates for micro- and nano-liter samples and especially pulsation-free flows are often the primary pump requirements for micro-flow injection analysis ( $\mu\text{-FIA}$ ), micro-column liquid chromatography ( $\mu\text{-LC}$ ), and other  $\mu\text{-TAS}$ . Micro-pumps that have been proposed for  $\mu\text{-TAS}$  can be classified as either field-induced flow pumps or mechanical membrane displacement pumps. Field-induced pumps include electro-osmotic flow (EOF) [1–3], electrohydrodynamic [4], centrifugal, and magneto-hydrodynamic pumps [5]; mechanical membrane displacement pumps include electrostatic, electromagnetic, thermo-pneumatic, photo-thermal, and piezoelectric pumps. A recent review paper describes recent advances in such micro-pumps [6]. The applications reported for electro-osmotic pumps (EOP) include pumping mobile phases in chromatography [7] and FIA [8] and integrating to mass spectrometers [9, 10]. Recently, our group reported an AC electro-kinetic micro-pump and micro-mixer design based on AC Faradaic polarization [11].

EOPs have several advantages over membrane displacement pumps. EOPs require no moving parts and

Z. Chen (✉) · P. Wang · H.-C. Chang  
Center for Microfluidics and Medical Diagnostics,  
Department of Chemical and Biomolecular Engineering,  
University of Notre Dame, 182 Fitzpatrick Hall,  
Notre Dame, IN 46556-5637, USA  
E-mail: zchen@nd.edu  
Tel.: +1574-631-5749  
Fax: +1574-631-8366

are cheap to fabricate. They are, therefore, disposable with the entire  $\mu$ -TAS unit. Because their flow is driven by an applied electric field, precise flow control can be achieved with a simple current or voltage-control circuit. However, conventional EOPs with an open channel or capillary suffer from two major problems. One is bubble generation, because of the large current in the open channel. In aqueous solutions, when the applied electrode potential exceeds a threshold of 1.1 V, significant electrolysis and other electrode reactions occur, producing ions that contaminate the sample [12] and generate bubbles, which block the micro-channels [13]. To eliminate this blockage, a bubble-releasing device is required downstream of the pump [7], or the electrodes are usually placed in isolated open reservoirs such that bubbles can escape and the ions cannot invade the flow channel [13]. However, the reservoir housing must be conducting to enable electric field penetration. An ion-selective conducting membrane that would not permit excessive ion leakage from the electrode reservoir has not been reported. It is generally believed that the solution to the reaction problem is to reduce the current by using dense packing [2, 14].

Another problem is that EOPs with an open channel or capillary generally have low stall pressures, and, therefore, are generally not used in systems with high-pressure loads. High-pressure build-up can be achieved only if the pump channel is smaller or if a dense packing material is used to produce large hydrodynamic resistance. Unlike mechanical pumps, which generate a local high pressure, and for which hydrodynamic resistance in the pump would reduce this driving pressure, pure EOF does not produce a pressure field but instead relies on hydrodynamic resistance to reduce the flow and build up a high pressure along the pump channel. Hence, in a counter-intuitive manner, EOP pump channels need to be as small as possible as but not smaller than the double layer thickness of the electrolyte. However, a single small pump channel cannot produce enough flow and a large bundle of small micro-channels is needed for EOP.

Because both the electrode reaction and the low-pressure disadvantages of EOPs can be reduced by dense packing within the pump channel, considerable effort has been devoted to fabrication of multiple micro-channels by lithography [9] or internal packing with high surface charge density that still allows EOF. One strategy is to pack the pump channel with small particles, for example chromatographic stationary phases [2, 7, 14]. The interstitial space between the particles in the packed column forms smaller multiple parallel channels. However, frits must be inserted at both ends of column to prevent particle movement and this insertion is difficult. Moreover, packing itself is a tedious and difficult procedure, especially when the capillary inner diameter is less than 100  $\mu\text{m}$ . Another new approach is to use monolithic materials. Frechet's group reported high-pressure EOPs based on porous polymer monoliths [15]. The authors pointed out that direct co-polymerization of functional monomers resulted in high and excessive

Joule heating. In addition, most of the ionizable groups were buried within the inaccessible polymer matrix rather than being exposed at the pore surface. As such, the packing is conducting but yields low EOF. Surface grafting was employed to introduce an ionizable functional moiety on to the surface of the monolith, a rather complicated fabrication procedure. As in capillary electrochromatography, polymeric monoliths also suffer from shrinking and swelling when exposed to fluids containing organic solvents.

Nakanishi's and Tanaka's groups pioneered the fabrication of silica rods for applications in chromatography [16, 17]. Previous work by Chen et al. demonstrated that the monolithic silica, with its high surface charge density, is a good column matrix for capillary electrochromatography (CEC) [18–21] and micro-liquid chromatography [22] for chiral separations, and for enzyme reactors immobilized with ascorbate oxidase for eliminating ascorbic acid during the monitoring of catecholamine [23]. This work showed that monolithic silica prepared by a sol-gel process has a continuous skeleton morphology with micrometer-sized through-pores and nano-porous surfaces on the skeleton. Silica-based monolith is superior to polymeric monolith in its mechanical strength and high stability in both aqueous and organic solution. Its surface charge can also be easily modified by use of different chemical functionality, to meet special requirements such as at low pH conditions. Therefore, this work is focused on the development of a novel monolithic EOP based on sol-gel process for micro flow analysis and electrospray.

With its high charge density, because of the dissociation of silanol group on the nano-porous skeleton, its low conductivity, and its micrometer-sized pores that result in large hydrodynamic resistance, silica monoliths should be an ideal EOP matrix. In addition to this new design, we use a Nafion joint in our downstream (cathode) electrode reservoir. Nafion is a conducting membrane but is not permeable to fluid flow. Thus the cathode is hydrodynamically isolated from the pump channel such that there is no flow exchange between the reservoir and the channel. The Nafion membrane hence offers even more hydrodynamic resistance and further enhances pump pressure. In addition, the Nafion membrane can prevent any bubbles generated in the reservoir from entering the flow channel, although negligible bubble generation is expected, because of the low current through the low-conducting monolith.

It has been demonstrated that an EOP with a 6-cm length of monolithic silica, prepared within a 100  $\mu\text{m}$  i.d. capillary, could generate a maximum pressure of 0.4 MPa at a maximum flow rate of 0.4  $\mu\text{L min}^{-1}$  at 6 kV. The measured current was below 100  $\mu\text{A}$  and no bubble generation and little pH change were detected at the electrodes, even when high electric field strength of 1,000  $\text{V cm}^{-1}$  was applied. This pump was integrated in a  $\mu$ -FIA system with an injector and a chemical sensor. It was shown that the monolithic EOP worked well as the fluid-driving unit for this  $\mu$ -FIA. In addition, we

demonstrated that, because of the high pressure and high field produced by the silica monolith, this pump could also work as an electro-spray to transfer the sample into a downstream mass spectrometer.

## Experimental

### Instrumentation

A  $\mu$ -FIA system was fabricated with a monolithic EOP, an injector, and an electrochemical detector (microchip sensor). Electrochemical measurement was carried out with Camry Instruments (Rack-Mount PC-520 system). The injector (Rheodyne 9125-080) was connected with a 10-cm length of capillary (i.d. 100  $\mu$ m) as the injection loop. Olympus 1X71 microscopy and i-speed CDU camera system (Olympus America) were used for recording and imaging the electro-spray. A HCZE-30PNO25-LD high-voltage power supply was purchased from Matsusada Precision Devices (Tokyo, Japan).

### Material and reagents

Fused-silica capillary tubing (100  $\mu$ m i.d. and 365  $\mu$ m o.d.) was obtained from Polymicro Technologies (Phoenix, USA) and used for making monolithic silica columns. Nafion tubing was obtained from Perma Pure (USA). Tetramethoxysilane (TMOS), poly(ethylene glycol) (PEG) (MW 10,000) and 3-hydroxytyramine hydrochloride (dopamine) were obtained from Aldrich (USA). Disodium ethylenediamine tetraacetate (EDTA), Tris(hydroxymethyl)aminomethane (Tris), sodium phosphate, and other chemical reagents were purchased from Fisher Scientific (USA). All solutions were prepared using distilled deionized (DI) water.

### Pump design and fabrication

The monolithic silica column was prepared with the same procedures as in Chen's previous works [18–23]. The morphology of monolithic silica was observed by scanning electron microscopy (SEM), as shown at the right bottom of Fig. 1. The monolithic silica has a continuous skeleton and micrometer-scale through-pores. Fig. 1 shows the design of the monolithic EOP. A 6 cm length of monolithic silica column was connected to a 3-cm length of open capillary by Nafion tubing, which was sealed with epoxy glue. The monolithic silica column connected with a capillary outlet was mounted on a 2.5 cm  $\times$  7.5 cm glass slide. Two 5-cm lengths of PVC tubing (8 mm o.d. and 5 mm i.d.) were glued on the slide as the reservoirs. One was located on the end of the monolith and another at the top of the junction of the Nafion tubing. When a positive high voltage was applied between the two reservoirs by means of a high-voltage power supply connected by platinum wire

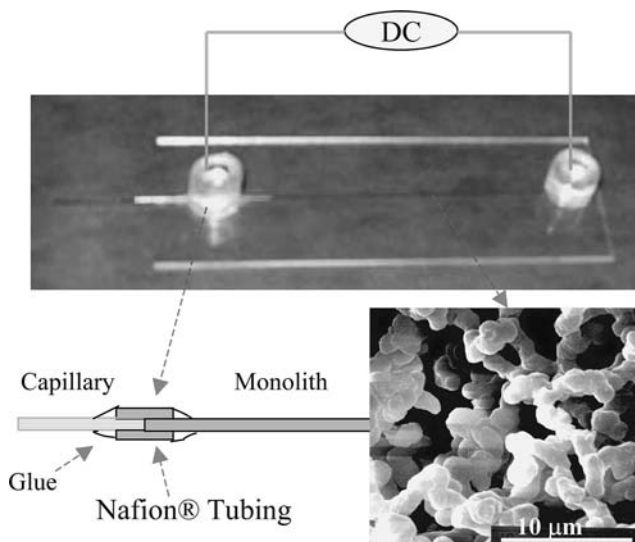


**Fig. 1** An image of the monolithic EOP, and an SEM picture of a monolith with a magnification of 5,000

electrodes, the fluid was pumped out the outlet of capillary because of the EOF generated within the through-pore channels.

## Results and discussion

### Characterization of monolithic EOP

EOP is, in principle, based on the EOF generated by the  $\zeta$  potential which forms as a result of the electrical double layer (EDL) at the solid/liquid interface. For glass or silica surfaces, deprotonation of acidic silanol groups produces a negatively charged surface. Counter ions from solution are attracted to the wall and shield these charges, with dissolved counter ions being repelled from the wall, forming the EDL. The characteristic thickness of the EDL is Debye shielding length,  $\lambda_D$ , of the ionic solution, given by:

$$\lambda_D = \left( \frac{\epsilon k T}{2 q^2 z^2 c} \right)^{1/2} \quad (1)$$

where  $\epsilon$  and  $T$  are the electrical permittivity and temperature of the solution, respectively,  $z$  and  $c$  are the valence number and average molar ion concentration, respectively,  $k$  is the Boltzmann constant, and  $q$  is the electron charge. When an electric field is applied, the mobile ions in the solution move in response to the field, dragging the bulk solution with them, and thereby producing EOF. The linear flow rate of EOF is expressed by the Smoluchowski slip velocity:

$$u_{\text{eof}} = -(\epsilon \zeta / \eta) E \quad (2)$$

Here  $u_{\text{eof}}$ ,  $\zeta$ ,  $\epsilon$ ,  $\eta$  and  $E$  are the EOF linear flow rate, the zeta potential at the capillary wall, the dielectric permittivity, the viscosity of the fluid, and the electric field applied across the capillary, respectively. The

electro-osmotic flux  $Q^*$  is related to  $u_{\text{eof}}$  and effective sectional area  $A$ , which is  $\pi a^2$  in a capillary of radius  $a$ , and can be expressed as:

$$Q^* = u_{\text{eof}}A = (\epsilon\zeta/\eta)E(\pi a^2) \quad (3)$$

However,  $Q^*$  is the pure EOF flow rate in the pump capillary without any pressure gradient. Because of flow balance, the flow rate in the pump must be equal to the flow in the micro-channels downstream. However, because there is no pressure build up, there is no flow downstream of the EOP. This dichotomy suggests that  $Q^*$  is not the flow rate within any pump channel with a load channel downstream. In fact, a positive pressure gradient is established within the pump channels to reduce its flow rate to  $Q$ . The pressure reaches a maximum at the Nafion joint and then decreases downstream in the load channel. This downstream negative pressure gradient drives the flow in the load channel such that it is equal to  $Q$ , the reduced flow rate in the pump.

If one models the monolithic silica as a bundle of independent capillaries (through-pores), the flow rate  $Q$  can be expressed as [12]:

$$Q = Q^*_{(a=r)} A - \frac{m\pi r^4 P_{\text{max}}}{8\eta L} \quad (4)$$

where  $P_{\text{max}}$  is the pressure at the end of the pump channel,  $L$  is the pump channel length,  $m$  is the number of effective pores (through pore) in the silica monolith, and  $r$  is the effective radius (through-pore) of the pump cross-sectional area such that the effective flow cross-section area  $A = m\pi r^2$ ,  $Q^* = \frac{\epsilon\zeta E}{\eta} m\pi r^2$ . On the basis of this equation it is clear that the pump pressure curve of  $P_{\text{max}}$  vs  $Q$  has a maximum flow rate of  $Q^*$  when  $P_{\text{max}}$  vanishes and a maximum of  $(8\eta L/r^2)Q^*$  at zero flow rate. This pressure curve is also linear. Relating this flow rate  $Q$  to the flow rate of a downstream load channel, which assumed to be an open cylindrical capillary of length  $L$  and radius  $R$ , we obtain:

$$Q = Q^* / [1 + m(L/L)(r/R)^2] \quad (5)$$

We wish to examine the effect of pore size  $r$  on the flow rate  $Q$ . The pure EOF flow  $Q^*$  scales  $r^2$  through the pump cross-section area  $A$  and hence approaches zero at low  $r$ . However, this reduction in pore-cross section area can be compensated by increasing the number of pores  $m$ . In fact, with a fixed flow cross-section area  $A$ , the pure EOF flow  $Q^*$  is fixed if we adjust the pore radius  $r$  while holding the cross-section porosity constant, because the Smoluchowski slip velocity  $u_{\text{eof}}$  is independent of the pore radius and its flow rate  $Q^*$  is hence proportional to the flow cross-sectional area  $A$ . Holding the porosity constant is a reasonable constraint as the porosity of the silica monolith is roughly constant while the pore size  $r$  can be varied by adjusting the pH, the sol-gel starting composition and PEG ratio [16–23]. The key  $r$  dependence hence enters only in the denominator of the flow rate in Eq. 5 if the porosity is held constant, where it accounts for the pressure build up in the pump

channel. Higher pressure and flow rate are thus achieved at low  $r$ . However, we should not reduce  $r$  less than the EDL thickness in Eq. 1. When  $r$  is less than  $\lambda_D$ , the Zeta potential  $\zeta$  scales linearly with respect to  $r$  and the flow rate again decreases with decreasing  $r$ . In fact, if  $r$  approaches nanometer levels and is much smaller than  $\lambda_D$ , flow penetration through the packing would become impossible. Thus, the key property dictating the performance of EOP is the pore radius  $r$  and it should be as small as possible but not smaller than  $\lambda_D$ .

We measured the flow rate by weighing the mass of fluid collected in a capillary (500  $\mu\text{m}$  i.d.) from the pump channel without a load for several minutes. Figure 2 shows the influence of the applied voltage on the flow rate and current. Both open-capillary and monolithic EOPs resulted in a linear relationship between flow rate and applied voltage, and between the current and applied voltage, which follows from the linearity of EOF with respect to the applied field, as seen in Eqs. 3 and 4. Comparing the flow rate and the current between open capillary and monolithic EOPs, it is known that both the flow rate and the current in open capillary EOP are near 2.5–3 times as high as those in monolithic EOP without a downstream load. This suggests that the effective cross-sectional area  $A$  of the monolith (through-pore) is about one-third of that for the open capillary. In other words, about two-thirds of the capillary is occupied by the monolithic silica skeleton, which would also be its porosity if one assumes the through pores are aligned longitudinally. Thus, the flow rate in the monolithic EOP is about one-third that of open capillary EOP. This also suggests that the power consumption of monolithic EOP is one third that of open capillary EOP. On the other hand, as indicated in Eq. 5, although the flow rate of open capillary EOP is higher than that of monolithic EOP, open capillary EOP does not generate high-pressure to drive flow in the downstream load channel. Monolithic EOP, with its small pore size and high

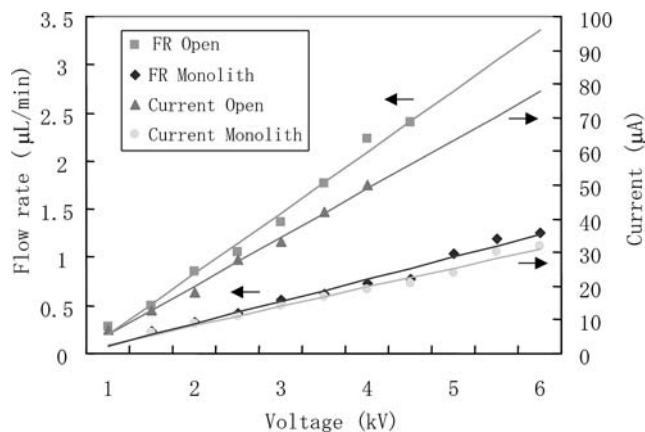


Fig. 2 Effect of applied voltage on flow rates and currents of monolithic pump and open capillary pump. 1.5 mmol L<sup>-1</sup> EDTA–0.26 mmol L<sup>-1</sup> Tris buffer: pH 6.0, conductance 5.0×10<sup>-4</sup> S cm<sup>-1</sup>

charge density, can generate high pressure to drive flow downstream in the load channel.

We measured the pump pressure curve of pressure  $P_{\max}$  vs flow rate  $Q$  of both monolithic EOP and open capillary EOP with a load by using the method of compressing air in an end-sealed capillary [1]. The pump curve in Fig. 3 is indeed linear as is consistent with Eq. 4 at different applied voltages (3, 5 and 6 kV). It can be seen from the curve that the monolithic EOP can generate pressure as high as 0.4 MPa when a potential of 6 kV was applied and when EDTA-Tris buffer was used as the test fluid. In contrast, the open capillary EOP did not generate any detectable pressure. Thus, the monolithic EOP, with its high pressure and low current, is ideal to drive flow against large loads in micro-systems such as  $\mu$ -LC,  $\mu$ -FIA, and microchip sensors. Zeng et al. [2] reported that particle-packed EOP suffered from severe hydrogen bubble generation in the low pressure range. However, Fig. 3 shows that our monolithic EOP does not have this problem. The minimum current of less than 100  $\mu$ A has reduced bubble generation to such an extent that they dissolve in the fluid during the duration of the experiment. Measurements of pH at the cathode reservoir also indicated little change in the pH during the experiment, again because of the small current and the stabilizing buffer solution. From Eq. 4, the slope of pump curve in Fig. 3, defined as  $k$ , should be equal to:  $8\eta L/m\pi r^4$ . Based on the plot of current vs voltage in Fig. 2, the effective cross-sectional area of the monolith ( $m\pi r^2$ ) is  $0.27\pi a^2$ , where  $a$  is radius of the open capillary used for preparing the monolith. Thus, we can obtain the average through-pore radius ( $r$ ):

$$r = \sqrt{\frac{8\eta L}{0.27\pi a^2 k}} \quad (6)$$

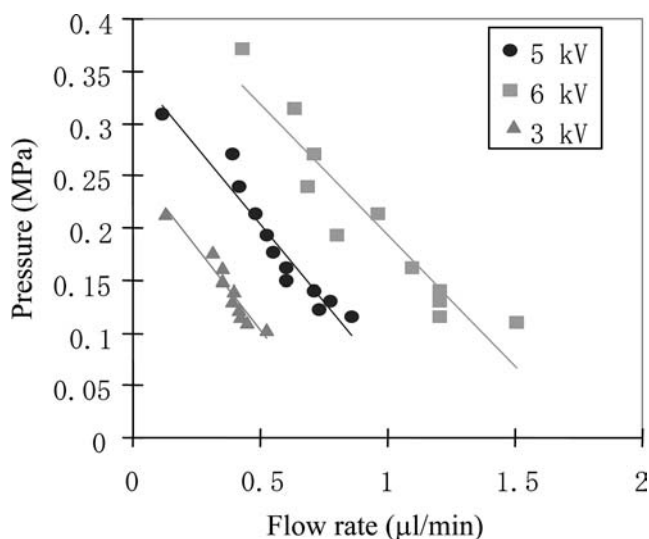


Fig. 3 Pressure vs flow rate curves of EOP at different applied voltages of 3, 5, and 6 kV. Running fluid: 1.5 mmol L<sup>-1</sup> EDTA–0.26 mmol L<sup>-1</sup> Tris buffer: pH 6.0, conductance:  $5.0 \times 10^{-4}$  S cm<sup>-1</sup>

Inserting the viscosity of water  $\eta = 1.0 \times 10^{-3}$  Pa s, pump length  $L = 6$  cm,  $a = 50$   $\mu$ m and the average slope of the pressure curves of  $k = 0.3$  MPa  $\mu$ L<sup>-1</sup> min from Fig. 3, the average through-pore radius  $r$  is estimated to be 3.5  $\mu$ m. This agrees with the observation by SEM in Fig. 1.

Figure 4 shows the relationship between the measured applied voltage and the flow rate with different working fluids, including DI water, EDTA-Tris buffer and organic solvents such as acetonitrile and methanol often used in reversed-phase LC (RP-LC). From Fig. 4 we can see that the flow rate of monolithic EOP can be adjusted by changing the applied voltage in the range 200 nL to 2.5  $\mu$ L min<sup>-1</sup>, depending on the type of fluid. On the basis of Eqs. 3 for  $Q^*$  and 5 for  $Q$ , the flow rate varies with the working fluid properties such as the ion density, pH, and viscosity that affect  $Q^*$ . In conclusion, the novel design of monolithic silica EOP and Nafion joint has overcome the main problems of low pressure and bubble interference in conventional open-capillary and packed EOP.

It should be mentioned that the EOF of the silica monolith depends on the fluid pH, because the negative charge on the silica surface arises primarily because of deprotonation of the silanol groups. It is known that the number of deprotonated silanol groups and hence the charge on the surface of silica monolith are greatly reduced under low-pH conditions, reaching a negligibly small value at a pH of around 2. Negligibly low surface charge translates into impractically low EOF. When delivering low-pH fluids it is recommended that a chemically modified silica monolith is used. We have demonstrated that an amino group-modified silica monolith generates strong anodic EOF under low pH conditions, because the NH<sub>2</sub> group associates with a proton and transfers the charge to NH<sub>3</sub><sup>+</sup> groups to produce a high surface positive charge under low pH conditions.

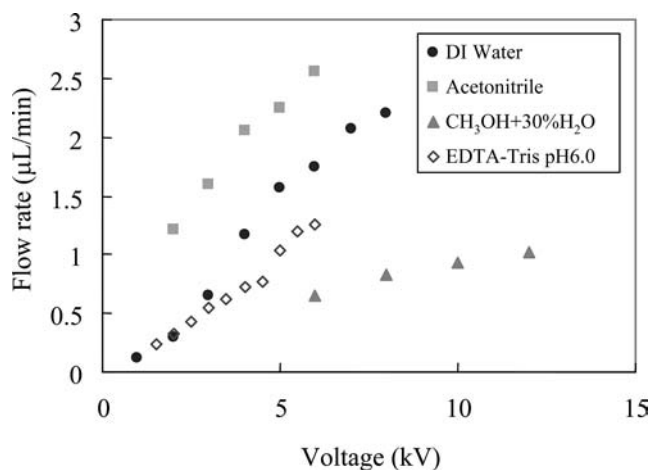
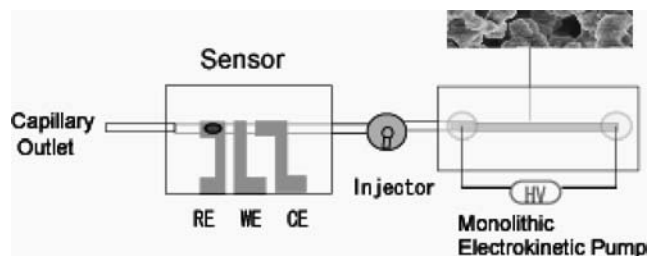


Fig. 4 Relationship between applied voltage and the flow rate for different fluids

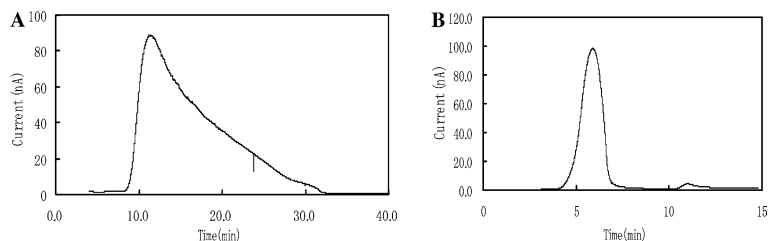


**Fig. 5** The  $\mu$ -FIA system consists of a monolithic EOP, an injector, and a microchip sensor with three carbon-film electrodes

### Application in $\mu$ -FIA

Micro flow analysis system like  $\mu$ -FIA,  $\mu$ -LC, and continuous monitoring on a microchip sensor requires the micro-pump to deliver fluid at micro or nano-liter flow rates consistent with our pump. As discussed in the "Introduction" section, EOP has many advantages over the mechanical pumps or syringe pumps used in conventional systems on larger scales. In this work we investigated the possibility of using monolithic EOP for  $\mu$ -FIA or  $\mu$ -LC. As shown in Fig. 5, monolithic EOP was integrated in a  $\mu$ -FIA system with a micro injector and a microchip sensor. The injector (Rheodyne 9125) was connected to 10 cm of open capillary loop (i.d. 100  $\mu$ m) to control the sample injection volume at approximately 0.8  $\mu$ L. The microchip sensor with three-electrode system was employed as an electrochemical detector. Teflon tubing was used to connect capillaries. The micro-sensor consisted of a carbon electrode substrate (25 mm $\times$ 15 mm), a cover glass (22 mm $\times$ 10 mm), and two capillaries for the inlet and outlet of the flow cell (365  $\mu$ m o.d. $\times$ 100  $\mu$ m i.d.) [23]. Carbon film electrodes (for a three-electrode system) were formed on a glass substrate by chemical vapor deposition (CVD) of an aromatic compound, photolithography, and dry etching. The electrodes were 0.5 mm apart. The area of the working electrode located in the center was 1 mm $\times$ 1 mm. The reference electrode was formed by coating the carbon-film electrode with Ag/AgCl paste.

**Fig. 6** Chronoamperometric curve of dopamine oxidation on microchip sensor in the  $\mu$ -FIA system with a Rheodyne injector (A), or a Teflon tube as injector (B). Phosphate buffer (1.0 mmol L<sup>-1</sup>): pH 8.0, conductance  $2.0 \times 10^{-4}$  S cm<sup>-1</sup>. Sample concentration: 0.1 mmol L<sup>-1</sup> dopamine in pH 8.0 in phosphate buffer



To connect the inlet and outlet capillaries, two channels approximately 5 mm from the inlet and outlet sides, 0.4 mm deep and 0.4 mm wide were cut in the cover glass by use of a dicing saw. The electrode substrate and cover glass were bonded together by use of double-sided tape with a thickness of 50  $\mu$ m. A 1 mm $\times$ 17 mm channel was created in the center of tape to form a flow cell with the inlet and outlet capillaries. These capillaries and the edges of the cover glass were sealed with a UV-curable resin.

A three-electrode system was used for the electrochemical measurements. The applied potential was 500 mV vs Ag/AgCl. The EOP flow rate was controlled by adjusting the applied voltage. An electro-active neurotransmitter, dopamine, was used as the test sample. Figure 6a shows chronoamperometric curve of dopamine oxidation on the microchip sensor in the  $\mu$ -FIA system. This result showed that monolithic EOP could be used as a fluid-driving unit for  $\mu$ -FIA. It was noticed in Fig. 6a that large dispersion was observed, with significant broadening and a long tail. This hydrodynamic dispersion is probably because of sample overload and a large dead volume of connecting capillaries downstream of the EOP. Although the 10 cm of capillary loop (i.d. 100  $\mu$ m) was calculated to have a 0.875  $\mu$ L injection volume, the dead volume of connections between the capillary and injector probably makes the actual injector volume much larger than 1  $\mu$ L. If a precisely volume-controlled injector with less than 1.0  $\mu$ L injection volume was used, a narrower peak would be expected. To test this idea we inserted the outlet of EOP and the capillary inlet of the sensor into 1 cm of Teflon tube (i.d. 365  $\mu$ m) filled with the sample solution, in place of the Rheodyne injector. As expected, a narrow peak was obtained, as shown in Fig. 6b. On the basis of these results, monolithic EOP can be used in  $\mu$ -FIA systems.

Recently, capillary electrophoresis (CE), micellar electrokinetic chromatography (MEKC), and CEC have been shown to be highly efficient micro-column separation techniques, because of the flat flow profile of EOF. However, micro-LC is still regarded as an important and indispensable separation technique for some samples that cannot employ CE, MEKC, and CEC. For example, if the stationary phase of the capillary column has high separation selectivity but cannot generate EOF, CEC is impossible. Micro-LC would remain the best selection. To examine the possibility of using monolithic EOP in  $\mu$ -LC, we connected monolithic EOP to a 40 cm monolithic silica column, and observed that the

electrolyte solution can be pumped through the monolithic column. Besides, as shown in Fig. 4, the monolithic EOP can deliver DI water, electrolytes, and organic solvents like acetonitrile and methanol, which are commonly used as the mobile phase in RP-LC. Thus, the monolithic EOP could be used for driving mobile phases in  $\mu$ -LC. Further study on the application for  $\mu$ -LC is in progress in our group.

### Electrosprays driven by EOP

Electro-spray is a convenient way of transmitting the sample from the micro-system into a downstream analytical instrument that cannot be integrated into the same substrate. Our group has recently developed an alternative AC spray technique [24]. AC sprays do not ionize the content of the spray and require a lower field than DC sprays. However, they produce a much larger drop ( $\sim 1 \mu\text{m}$ ) and hence are not suitable for mass spectrometer applications. The large field and pressure produced by our EOP suggests that it could be used to interface the substrate with mass spectrometry. In our recent studies on DC electro-spray, both pressure and flow rate were shown to sensitively affect the critical field for spraying to occur and the stability of the DC spray. In some studies, external mechanical syringe pumps were usually connected with the metal needle electrode for transporting the fluid at  $\text{nL-}\mu\text{L h}^{-1}$  flow rates to the tip of needle, so that the fluid can be ejected in the form of a spray [25, 26]. However, flow rate and pressure are not analogous and hence it is not clear that electro-spray is being enhanced by the introduced flow.

When a negative voltage higher than a critical value of  $3.5 \text{ V cm}^{-1}$  was applied on our monolithic EOP, as shown in Fig. 7, a stable DC electro-spray was observed. The image obtained from high-speed video camera with microscopy in Fig. 8 shows a stable Taylor cone and a nano-jet of emitted spray. The anode is grounded to maintain the same field direction within the monolith—to generate the usual EOF toward the cathode.

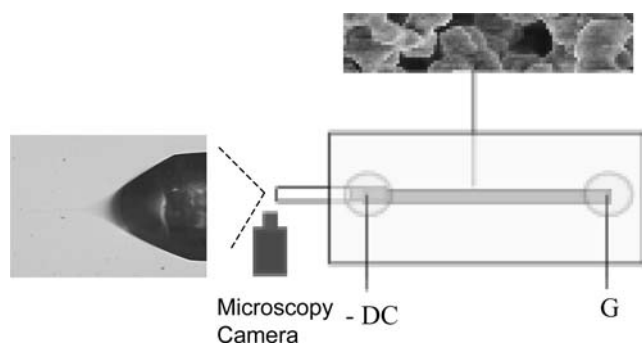


**Fig. 7** Schematic microdevice which functions as both EOP and ES. A microscope with a high-speed digital camera is set at the tip of capillary to record the image of the electro-spray



**Fig. 8** An image of the stable Taylor cone and nano-fluidic jet of the electro-spray. Fluid EDTA-Tris; potential 3.5 kV; capillary: i.d. 100  $\mu\text{m}$ , o.d. 365  $\mu\text{m}$

However, the negative voltage at the cathode ensures the extension of field lines beyond the cathode toward the grounded infinity. These extended field lines sustain the electro-spray at the capillary outlet. If the cathode is grounded and a positive voltage is applied at the anode, the fluid is pumped out but spraying is not observed. The electro-spray based on our monolithic EOP functioned for both aqueous solutions and organic solvents, such as acetonitrile and methanol. Regulating the applied voltage can transform the ejected stream from a continuous jet into discontinuous droplets, thus enabling fluid transmission at different rates. This EOP spray is also expected to be used in mass spectrometric analysis and in the material sciences for making nano- or micro- materials.

### Conclusions

In this work we have successfully developed a novel EOP based on highly charged and monolithic silica with micrometer-sized through pores. This monolithic EOP can generate a stable high pressure to drive a precise flow through large downstream loads. The Nafion joint for the electrode reservoir further enhances the pressure to as high as 0.4 MPa. When this pump was used as a fluid-driving unit in a  $\mu$ -FIA system it worked well as a substitute for larger mechanical pumps in conventional FIA systems. When a negative voltage was applied to the pump, the high pressure produces an electro-spray at relatively low fields to enable interfacing with a downstream analytical instrument.

**Acknowledgments** We thank Dr Albert E. Miller, University of Notre Dame, for use of his electrochemical instrument; Dr William Boggess, University of Notre Dame, for the injector used in this study, and Mr Katsuyashi Hayashi, NTT Microsystem Integration Labs, for valuable discussion on the sensor. This work is supported by the Center for Microfluidics and Medical Diagnostics at the University of Notre Dame.

---

**References**

1. Chen CH, Santiago JG (2002) *J Microelectromech Syst* 11:672–683
2. Zeng S, Chen CH, Mikkelsen JC, Santiago JG (2001) *Sens Actuators B* 79:107–114
3. Morf WE, Guenat OT, Rooij NF (2001) *Sens Actuators B* 72:266–272
4. Darabi J, Rada M, Ohadi MM, Lawler J (2002) *J Microelectromech Syst* 11:684–690
5. Lemoff AV, Lee AP (2000) *Sens Actuators B* 63:178–185
6. Laser DJ, Santiago JG (2004) *J Micromech Microeng* 14:R35–R64
7. Chen L, Ma J, Guan Y (2003) *Microchem J* 75:15–21
8. Liu S, Dasgupta PK (1992) *Anal Chim Acta* 268:1–6
9. Lazar IM, Karger BL (2002) *Anal Chem* 74(24):6259–6268
10. Lazar IM, Ramsey RS, Jacobson SC, Foote RS, Ramsey JM (2000) *J Chromatogr A* 892:195–201
11. Lastochkin D, Zhou R, Wang P, Ben Y, Chang H-C (2004) *J Appl Phys* 96:1730–1733
12. Minerick AR, Ostafin AE, Chang H-C (2002) *Electrophoresis* 23:2165
13. Mutlu S, Yu C, Selvaganapathy P, Svec F, Mastrangelo CH, Frechet JMJ (2002) In: *Proceedings of the IEEE MEMS 2002 Conference, Las Vegas, USA, Jan 20–24*, pp 19–24
14. Razunguzwa TT, Timperman AT (2004) *Anal Chem* 76:1336–1341
15. Tripp JA, Svec F, Frechet JMJ, Zeng SL, Mikkelsen JC, Santiago JG (2004) *Sens Actuators B* 99:66–73
16. Nakanishi KJ (1997) *Porous Mater* 4:67–112
17. Tanaka N, Kobayashi H, Nakanishi K, Minakuchi H, Ishizuka N (2001) *Anal Chem* 73(15):420A–429A
18. Chen Z, Hobo T (2001) *Anal Chem* 73:3348–3357
19. Chen Z, Hobo T (2001) *Electrophoresis* 22:3339–3346
20. Chen Z, Ozawa H, Uchiyama K, Hobo T (2003) *Electrophoresis* 24:2550–2558
21. Chen Z, Nishiyama T, Uchiyama K, Hobo T (2004) *Anal Chim Acta* 501:17–23
22. Chen Z, Uchiyama K, Hobo T (2002) *J Chromatogr A* 924:83–91
23. Chen Z, Hayashi K, Ywasaki Y, Kurita R, Niwa O, Sunagawa K (2005) *Electroanalysis* 17:231–238
24. Yeo LY, Lastochkin D, Wang SC, Chang H-C (2004) *Phys Rev Lett* 92:133902–133904
25. Lasen G, Velarde-Ortiz R, Minchow K, Barrero A, Loscertales LG (2003) *J Am Chem Soc* 125:1154–1155
26. Loscertales IG, Barrero A, Guerrero I, Cortijo R, Marquez M, Ganán-Calvo AM (2002) *Science* 295:1695